

National Bureau of Standards

Library, N. W. Bldg.

NOV 16 1949

NATIONAL BUREAU OF STANDARDS
CENTRAL RADIO PROPAGATION LABORATORY
WASHINGTON, D. C.

THEORY AND DESIGN OF A WAVEGUIDE
BELOW CUTOFF ATTENUATOR

BY J. J. FREEMAN

THEORY AND DESIGN OF A WAVEGUIDE BELOW CUT-OFF ATTENUATOR

By J. J. FREEMAN

ABSTRACT

The fields generated by an arbitrary current distribution exciting a piston-type attenuator are developed, and symmetric distributions exciting maximum amplitudes of the dominant mode, and minimum amplitudes of unwanted modes are investigated. The relative error in voltage measurement due to spurious modes is computed as a function of spacing between exciting and receiving coils for certain simple current distributions. The relative merits of circular and rectangular attenuator cross-sections are discussed.

I. Introduction

The waveguide below cut-off attenuator, also known as a piston or mutual inductance type attenuator, was first designed by Wheeler, Harnett and Case¹ for use in signal generators, and has since found wide application. The method consists in exciting a hollow tube below its cut-off frequency and receiving the attenuated field by means of a coil or condenser. Since the generated electromagnetic field falls off exponentially with distance from the exciting source, and since the attenuation constant may be computed from the dimensions of the tube, the ratio of any two voltages is reduced to a measurement of length.

Preparatory to the design and construction of such an attenuator, it was thought advisable to investigate the theory to determine the kind of excitation required for optimum mode purity, and an evaluation of the amplitudes of the unwanted modes, for different types of excitation. A

rigorous solution of the problem is impossible, but an approximate solution which is useful consists in determining the field produced by an arbitrary current distribution within a waveguide closed at both ends. Here the perturbation of the field by the receiving loop is neglected.

Thus, given a distribution of current density, $\underline{J}(x', y', z')e^{-j\omega t}$, we seek the field produced within a perfectly conducting cavity. The scalar analogue, where $\underline{J}(x', y', z')$ is replaced by ρ , the charge density, is well known, and has been treated elegantly by Sommerfeld². The vector problem is solved analogously, by expansion into orthogonal vector wave functions, and has been treated by Heitler³, Condon⁴, and others. For completeness, the method is outlined below.

2. Expansion of the Field into Normal Vector Functions.

We use MKS units, and assume the fields and source vary as $e^{-j\omega t}$

Then, according to Maxwell's equations⁵, we must find a solution of

$$\nabla \times \nabla \times \underline{E} - k^2 \underline{E} = j\omega\mu \underline{J} \quad (1)$$

subject to the boundary condition that $\underline{n} \times \underline{E} = 0$, on the surface S , of the cavity where \underline{n} is the normal on S . \underline{E} is the electric field, and \underline{J} the impressed current density. Since any vector field may be shown to consist of two parts, one of zero curl, and the other of zero divergence, let $\underline{J} = \underline{J}_1 + \underline{J}_2$, where $\text{curl } \underline{J}_1 = 0$, and $\text{div } \underline{J}_2 = 0$.

$$\text{Then } \underline{J}_1 = \nabla \phi$$

Let $\underline{E} = \underline{E}_1 + \underline{E}_2$, where $\text{curl } \underline{E}_1 = 0$, and $\text{div } \underline{E}_2 = 0$.

$$\text{Then } \underline{E}_1 = \nabla \Psi$$

$$\text{curl}^2 \underline{E}_2 - k^2 \underline{E}_2 = j\omega\mu \underline{J}_2 \quad (2)$$

$$\underline{E}_1 = - \frac{j\omega\mu}{k^2} \underline{J}_1 \quad (3)$$

If Ψ_α is a solution of $\nabla^2 \Psi_\alpha + k_\alpha^2 \Psi_\alpha = 0$, and $\Psi_\alpha = 0$ on S, the interior surface of the cavity, $\nabla \Psi_\alpha \times \underline{n} = 0$ on S. If the Ψ_α are normalized, and orthogonal, then $\frac{1}{k_\alpha} \nabla \Psi_\alpha$ are normalized and orthogonal, since

$$\int \nabla \Psi_\alpha \cdot \nabla \Psi_\beta d\tau = \int (\nabla \cdot [\Psi_\beta \nabla \Psi_\alpha] - \Psi_\beta \nabla^2 \Psi_\alpha) d\tau = k_\alpha^2 \int \Psi_\alpha \Psi_\beta d\tau$$

Here $d\tau$ is an element of volume, and the integration is performed throughout the volume of the cavity.

Then if we call the normalized $\frac{1}{k_\alpha} \nabla \Psi_\alpha = \underline{E}_\alpha$, an arbitrary irrotational vector function whose tangential component vanishes on S may be developed in terms of the \underline{E}_α .

Thus,

$$\underline{E}_1 = \sum_\alpha a_\alpha \underline{E}_\alpha$$

$$\text{where } a_\alpha = \int \underline{E}_1 \cdot \underline{E}_\alpha d\tau$$

$$\underline{J}_1 = \sum_\alpha \int \underline{J}_1 \cdot \underline{E}_\alpha d\tau \underline{E}_\alpha$$

Substituting the above values of \underline{E}_1 and \underline{J}_1 in (3).

$$\underline{E}_1(r) = - \frac{j\omega\mu}{k^2} \sum_\alpha \int \underline{J}_1(r') \cdot \underline{E}_\alpha(r') d\tau' \underline{E}_\alpha(r) \quad (4)$$

If we had a complete set of orthogonal vector wave functions, \underline{E}_β , and if $\text{div } \underline{E}_\beta = 0$, and $\underline{n} \times \underline{E}_\beta = 0$, an arbitrary solenoidal vector, whose tangential component vanished on S, in particular \underline{E}_2 , could be expanded in terms of the \underline{E}_β . Suppose the \underline{E}_β are solutions of

$$\text{curl}^2 \underline{E}_\beta - k_\beta^2 \underline{E}_\beta = 0,$$

where $\underline{n} \times \underline{E}_\beta = 0$, and $\text{div } \underline{E}_\beta = 0$. Then it may be shown that the \underline{E}_β are orthogonal to each other, and to the \underline{E}_α .

$$\text{Let } \underline{E}_2 = \sum_\beta e_\beta \underline{E}_\beta, \text{ and let } \underline{J}_2 = \sum_\beta j_\beta \underline{E}_\beta$$

$$\text{Then, } j_\beta = \int \underline{J}_2 \cdot \underline{E}_\beta d\tau$$

Substituting the above values for \underline{E}_2 and \underline{J}_2 in Eq. (2),

$$e_\beta = \frac{j \omega \mu}{k_\beta^2 - k^2} \int \underline{J}_2 \cdot \underline{E}_\beta d\tau \quad (5)$$

$$\underline{E}_2 = j \omega \mu \sum_\beta \frac{\int \underline{J}_2(r') \cdot \underline{E}_\beta(r') d\tau'}{(k_\beta^2 - k^2)} \underline{E}_\beta(r)$$

Since the \underline{E}_α are orthogonal to the \underline{E}_β , and the \underline{E}_α and \underline{E}_β are assumed complete for expansions of electric fields of zero curl and zero divergence, respectively, $\int \underline{J}_2 \cdot \underline{E}_\alpha d\tau = \int \underline{J}_1 \cdot \underline{E}_\beta d\tau = 0$. Accordingly, we may drop the subscripts in \underline{J}_1 and \underline{J}_2 in Eq. (4) and (5), and substitute the total current density, \underline{J} .

$$\text{Thus, } \underline{E}_1(r) = \frac{-j \omega \mu}{k^2} \sum \int \underline{J}(r') \cdot \underline{E}_\alpha(r') d\tau' \underline{E}_\alpha(r) \quad (6)$$

$$\underline{E}_2(r) = j \omega \mu \sum \frac{\int \underline{J}(r') \cdot \underline{E}_\beta(r') d\tau'}{(k_\beta^2 - k^2)} \underline{E}_\beta(r)$$

3. Attenuators of Circular Cross-Section

We consider now the normal vector modes for the circular cylinder of radius a , and length d , where \underline{i}_1 , \underline{i}_2 and \underline{k} are the unit vectors in the directions of increasing r , θ and z .

Orthogonal vector wave functions have been treated by Stratton⁶, and the normal vector modes are most easily obtained by following his treatment, and satisfying the appropriate boundary conditions. For the interior of a circular cylinder,

$$\underline{E}_\alpha = \underline{E}_{\alpha 0} = \frac{F_{nm}^0}{\sqrt{\lambda_{nm}^2 + \frac{1^2 \pi^2}{d^2}}} \left[\begin{aligned} & \left\{ \lambda_{nm} J'_n(\lambda_{nm} r) \left(\frac{\cos n\theta}{\sin n\theta} \right) \underline{i}_1 \right. \\ & \left. + \frac{n}{r} \left(\frac{-\sin n\theta}{\cos n\theta} \right) J_n(\lambda_{nm} r) \underline{i}_2 \right\} \sin \frac{1}{d} \pi z + \left(\frac{\cos n\theta}{\sin n\theta} \right) J_n(\lambda_{nm} r) \frac{1}{d} \pi \cos \frac{1}{d} \pi z \underline{k} \end{aligned} \right] \quad (7)$$

Here, $\lambda_{nm} = \frac{u_{nm}}{a}$, where $J_n(u_{nm}) = 0$. (8)

and $k_\alpha^2 = k_{nm}^2 = \lambda_{nm}^2 + \left(\frac{1}{d} \pi \right)^2$ (9)

The normalizing factor, F_{nm} is

$$F_{nm}^0 = \left(\frac{\sqrt{4 - 2\delta_n^0}}{\sqrt{4 - 4\delta_n^0}} \right) \frac{1}{a \sqrt{\pi d} |J_{n-1}(\lambda_{nm} a)|} \quad (10)$$

The normal vector modes \underline{E}_β , consist of two independent, mutually orthogonal sets, the transverse electric type, which we designate as \underline{M}_β , and the transverse magnetic type, which we designate as \underline{N}_β .

$$\underline{M}_\beta = \underline{M}_{nm0}^e = A_{nm0}^e \left[\frac{n}{r} \left(\frac{-\sin n\theta}{\cos n\theta} \right) J_n(\delta_{nm} r) \underline{i}_1 - \delta_{nm} J_n'(\delta_{nm} r) \left(\frac{\cos n\theta}{\sin n\theta} \right) \underline{i}_2 \right] \times \sin \frac{1\pi z}{d} \quad (11)$$

Here, $\delta_{nm} = \frac{v_{nm}}{a}$, $J_n'(v_{nm}) = 0$

and $k_{nml}^2 = \delta_{nm}^2 + \left(\frac{1\pi}{d} \right)^2$ (12)

The normalizing factor is

$$A_{nm0}^e = \frac{2}{\sqrt{\pi d(1+\delta_0^n)} \sqrt{v_{nm}^2 - n^2} J_n(v_{nm})} \quad (12a)$$

$$\underline{N}_\beta = \frac{F_{nm0}^e}{\lambda_{nm} \sqrt{\lambda_{nm}^2 + \frac{1^2 \pi^2}{d^2}} \sqrt{1+\delta_0^n}} \left[\frac{-1\pi}{d} \sin \frac{1\pi z}{d} \left\{ \left(\frac{\cos n\theta}{\sin n\theta} \right) \lambda_{nm} J_n'(\lambda_{nm} r) \underline{i}_1 + \frac{n}{r} \left(\frac{-\sin n\theta}{\cos n\theta} \right) J_n(\lambda_{nm} r) \underline{i}_2 \right\} + \lambda_{nm}^2 \cos \frac{1\pi z}{d} J_n(\lambda_{nm} r) \left(\frac{\cos n\theta}{\sin n\theta} \right) \underline{k} \right] \quad (13)$$

When no ambiguity results, we shall omit the subscripts 1, m, n, and write λ_{nm} , for instance, as λ . We also omit the even, odd designations ($_0^e$), and write m_0^e as n, the even, odd designation being implied.

Substituting (11) and (13) in (6),

$$\underline{E}_2 = j\omega\mu \sum_{n,m,1} \frac{\underline{J}(r') \cdot \underline{M}(r') d\tau' \underline{M}(r)}{\delta^2 + \left(\frac{1\pi}{d} \right)^2 - k^2} + j\omega\mu \sum_{n,m,1} \frac{\underline{J}(r') \cdot \underline{N}(r') d\tau' \underline{N}(r)}{\lambda^2 + \left(\frac{1\pi}{d} \right)^2 - k^2} \quad (14)$$

Call the first summation \underline{A} , the second \underline{B} , so that

$$\underline{E}_2 = \underline{A} + \underline{B}$$

Let $\underline{M}_{nml} = A_{nm} m_{nm} \sin \frac{1\pi z}{d}$

where $m_{nm}^e = \frac{n}{r} \left(\frac{-\sin n\theta}{\cos n\theta} \right) J_n(\delta r) \underline{i}_1 - \left(\frac{\cos n\theta}{\sin n\theta} \right) \delta J_n'(\delta r) \underline{i}_2$

Then

$$\underline{A} = j\omega\mu \sum_{n,m} A_{nm}^2 \int \underline{J}(\underline{r}') \cdot \underline{m}(\underline{r}') \underline{m}(\underline{r}) \sum_{l=1}^{\infty} \frac{\sin \frac{1}{d} \pi z' \sin \frac{1}{d} \pi z}{\delta^2 - k^2 + \left(\frac{1}{d}\right)^2} d\tau' \quad (15)$$

In Appendix I, it is shown that

$$\sum_{l=1}^{\infty} \frac{\sin \frac{1}{d} \pi z' \sin \frac{1}{d} \pi z}{\delta^2 - k^2 + \left(\frac{1}{d}\right)^2} = S_1 = \frac{d}{2\gamma} \sinh \gamma z' \left(\frac{1 - e^{-2\gamma(d-z)}}{1 - e^{-2\gamma d}} \right) e^{-\gamma z}$$

$$\text{where } \gamma_{nm} = \sqrt{\frac{v_{nm}^2}{a^2} - k^2}$$

Substituting the above in (15), and substituting the value of A_{nm} given in (12a).

$$\underline{A} = j\omega\mu \sum_{n=0}^{\infty} \sum_{m=1}^{\infty} \frac{2e^{-\gamma z} \left(\frac{1 - e^{-2\gamma(d-z)}}{1 - e^{-2\gamma d}} \right)}{\pi (1 + \delta_0^n) (v_{nm}^2 - n^2) J_n^2(v_{nm}) \gamma} \int \underline{J}(\underline{r}') \cdot \underline{m}(\underline{r}') \underline{m}(\underline{r}) \sinh \gamma z' d\tau' \quad (16)$$

Let

$$\underline{D}_{nm}^e = \left[-\lambda_{nm} J'_n(\lambda_{nm}) \begin{pmatrix} \cos n\theta \\ \sin n\theta \end{pmatrix} \underline{i}_1 + \begin{pmatrix} \sin n\theta \\ -\cos n\theta \end{pmatrix} \frac{n}{\lambda} J_n(\lambda_{nm}) \underline{i}_2 \right] \quad (17)$$

and

$$\underline{p}_{nm}^e = \begin{pmatrix} \cos n\theta \\ \sin n\theta \end{pmatrix} J_n(\lambda_{nm}) \underline{k} \quad (18)$$

Substituting (17) and (18) in the second sum of (14), we get

$$\underline{B} = j\omega\mu \int \underline{J}(\underline{r}') \cdot \sum_{n,m} \frac{\underline{F}_{nm}^e}{\lambda^2} \left\{ \underline{n}(\underline{r}') \underline{n}(\underline{r}) \sum_{l=1}^{\infty} \frac{\left(\frac{1}{d}\right)^2 \sin \frac{1}{d} \pi z' \sin \frac{1}{d} \pi z}{\left(\lambda^2 + \frac{1^2 \pi^2}{d^2}\right) \left(\lambda^2 - k^2 + \frac{1^2 \pi^2}{d^2}\right)} \right. \quad (19)$$

$$\left. + \lambda^2 \underline{n}(\underline{r}') \underline{p}(\underline{r}) \sum_{l=1}^{\infty} \frac{\frac{1}{d} \sin \frac{1}{d} \pi z' \cos \frac{1}{d} \pi z}{\left(\lambda^2 + \frac{1^2 \pi^2}{d^2}\right) \left(\lambda^2 - k^2 + \frac{1^2 \pi^2}{d^2}\right)} + \lambda^2 \underline{p}(\underline{r}') \underline{n}(\underline{r}) \sum_{l=1}^{\infty} \frac{\frac{1}{d} \cos \frac{1}{d} \pi z' \sin \frac{1}{d} \pi z}{\left(\lambda^2 + \frac{1^2 \pi^2}{d^2}\right) \left(\lambda^2 - k^2 + \frac{1^2 \pi^2}{d^2}\right)} \right\}$$

$$+ \chi^4 \underline{p}(\kappa') \underline{p}(\kappa) \sum_{l=0}^{\infty} \frac{\cos \frac{l\pi z'}{d} \cos \frac{l\pi z}{d}}{\left(\chi^2 + \frac{l^2 \pi^2}{d^2}\right) (1 + \delta_0^l) \left(\chi^2 - k^2 + \frac{l^2 \pi^2}{d^2}\right)} \Bigg\} d\tau'$$

Similarly, if we substitute eq. 17, 18, and 7 in eq. 6,

$$\begin{aligned} \underline{E}_1 = & -\frac{j\omega\mu}{k^2} \int \underline{J}(\kappa') \cdot \sum_{n,m} F_{nm}^2 \left\{ \underline{n}(\kappa') \underline{n}(\kappa) \sum_{l=1}^{\infty} \frac{\sin \frac{l\pi z'}{d} \sin \frac{l\pi z}{d}}{\chi^2 + \frac{l^2 \pi^2}{d^2}} \right. \\ & - \underline{n}(\kappa') \underline{p}(\kappa) \sum_{l=1}^{\infty} \frac{\frac{l\pi}{d} \sin \frac{l\pi z'}{d} \cos \frac{l\pi z}{d}}{\chi^2 + \frac{l^2 \pi^2}{d^2}} - \underline{p}(\kappa') \underline{n}(\kappa) \sum_{l=1}^{\infty} \frac{\frac{l\pi}{d} \cos \frac{l\pi z'}{d} \sin \frac{l\pi z}{d}}{\chi^2 + \frac{l^2 \pi^2}{d^2}} \\ & \left. + \underline{p}(\kappa') \underline{p}(\kappa) \sum_{l=1}^{\infty} \frac{\frac{l^2 \pi^2}{d^2} \cos \frac{l\pi z'}{d} \cos \frac{l\pi z}{d}}{\chi^2 + \frac{l^2 \pi^2}{d^2}} \right\} d\tau' \end{aligned} \quad (20)$$

With a little manipulation, \underline{E}_1 and \underline{B} may be combined to give

$$\begin{aligned} \underline{E}_1 + \underline{B} = & \frac{j}{\omega \epsilon} \int \underline{J}(\kappa') \cdot \sum_{n,m} F^2 \left\{ \underline{n}(\kappa') \underline{n}(\kappa) \frac{k^2 - \chi^2}{\chi^2} \sum_{l=1}^{\infty} \frac{\sin \frac{l\pi z'}{d} \sin \frac{l\pi z}{d}}{\chi^2 - k^2 + \frac{l^2 \pi^2}{d^2}} \right. \\ & + \underline{n}(\kappa') \underline{p}(\kappa) \sum_{l=0}^{\infty} \frac{\frac{l\pi}{d} \sin \frac{l\pi z'}{d} \cos \frac{l\pi z}{d}}{\chi^2 - k^2 + \frac{l^2 \pi^2}{d^2}} + \underline{p}(\kappa') \underline{n}(\kappa) \sum_{l=1}^{\infty} \frac{\frac{l\pi}{d} \cos \frac{l\pi z'}{d} \sin \frac{l\pi z}{d}}{\chi^2 - k^2 + \frac{l^2 \pi^2}{d^2}} \\ & \left. + \underline{p}(\kappa') \underline{p}(\kappa) \sum_{l=0}^{\infty} \left(k^2 - \frac{l^2 \pi^2}{d^2} \right) \frac{\cos \frac{l\pi z'}{d} \cos \frac{l\pi z}{d}}{\left(\chi^2 - k^2 + \frac{l^2 \pi^2}{d^2}\right) (1 + \delta_0^l)} \right\} d\tau' \end{aligned} \quad (21)$$

Thus, the contribution to the field from \underline{E}_1 is exactly equal and opposite to part of the contribution arising from \underline{B} , so that the total field may now be divided into two parts, a transverse electric field, \underline{E}_{TE} , which corresponds at low frequencies to inductive coupling, and a transverse magnetic field, \underline{E}_{TM} , which corresponds at low frequencies to capacitive coupling.

$$\text{Thus, } \underline{E}_{TE} = \underline{A}$$

$$\underline{E}_{TM} = \underline{E}_1 + \underline{B}$$

$$\underline{E}_{\text{Total}} = \underline{E}_{TE} + \underline{E}_{TM}$$

The various infinite sums are evaluated in Appendix I and II. When the values of these summations are substituted in eq. 15 and 21, we get

$$\underline{E}_{TE} = \underline{A} = j\omega\mu \sum_{n=0}^{\infty} \sum_{m=1}^{\infty} \frac{2e^{-\gamma_{nm}Z}(1-e^{-2\gamma_{nm}(d-Z)})}{\pi(1+\delta_0^n)(V_{nm}^2-n^2)J_n^2(V_{nm})\gamma_{nm}(1-e^{-2\gamma_{nm}d})} \left[\int \underline{J}(\kappa') \cdot \underline{m}_{nm}^e(\kappa') m_{nm}^e(\kappa) \sinh \gamma_{nm}Z' d\tau' \right] \quad (22)$$

$$\underline{E}_{TM} = \underline{E}_1 + \underline{B} = -\frac{j}{\omega\epsilon} \sum_{n=0}^{\infty} \sum_{m=1}^{\infty} \frac{(2-\delta_0^n)e^{-\eta_{nm}Z}}{\pi U_{nm}^2 J_{n-1}^2(U_{nm})(1-e^{-2\eta_{nm}d})} \left[\right]$$

$$(1-e^{-2\eta_{nm}(d-Z)}) \int \underline{J}(\kappa') \cdot \left[\underline{n}_{nm}(\kappa') \underline{n}_{nm}(\kappa) \eta_{nm} \sinh \eta_{nm}Z' - \chi_{nm}^2 \underline{p}_{nm}(\kappa') \underline{n}_{nm}(\kappa) \cosh \eta_{nm}Z' \right] d\tau'$$

$$+ (1 + e^{-2\gamma_{nm}(d-z)}) \int \underline{J}(\lambda') \cdot \left[\chi_{nm}^2 \underline{\rho}_{nm}(\lambda') \underline{p}(\lambda) \sinh \gamma_{nm} z' - \chi_{nm}^4 \underline{p}_{nm}(\lambda') \underline{p}(\lambda) \frac{\cosh \gamma_{nm} z'}{\gamma_{nm}} \right] d\tau' \quad (23)$$

where $\gamma_{nm} = \sqrt{\chi_{nm}^2 - k^2}$

We notice first that the various modes are either in phase or 180° out of phase, which is, of course necessary, since we have neither resistive nor radiation losses. Also, the field does not decrease exponentially with z , but contains a factor, $(1 \pm e^{-2\gamma(d-z)})$ which is insignificant at small values of attenuation, but becomes appreciable as the receiving loop approaches the end of the cavity. If the attenuator were used in this way, its calibration in decibels would not be linear with variation of z . This non-linearity can be avoided if the attenuator is constructed as illustrated in Fig. 1. The exciting loop is fixed relative to a fixed end of the cavity, and the receiving loop is fixed to the other end which may slide within the cavity, varying its length, so that $d - z$ is a constant. Since $e^{-2\gamma d} \ll 1$, the denominator is independent of d and the ratio of E_{TE} for a given mode, for two positions of the receiving loop, z_1 and z_2 , is $e^{-\gamma(z_1 - z_2)}$, and the non-linearity is eliminated.

A variable contact between piston and attenuator wall (Fig. 1)

effectively varies the attenuator length d , which enters in the expression for the field in the factor $(1 \pm e^{-2\gamma(d-z)})$. Thus, the effect of a variable contact at A can be minimized by choosing a value of $d - z$ such that $e^{-2\gamma(d-z)} \ll 1$. Accordingly, a preferred design of piston is as indicated in Fig. 2, where the contact between piston and wall is made behind the receiving loop.

In general, an infinite number of modes are excited, so that the best one can do to insure purity of mode is to use symmetry of excitation which will not excite those unwanted modes with the lowest attenuation factor, and to use large enough values of z , such that the unwanted modes are sufficiently attenuated.

For low enough frequency,

$$\gamma_{nm} = \sqrt{\frac{V_{nm}^2}{a^2} - k^2} \approx \frac{V_{nm}}{a}, \text{ where } J'_n(V_{nm}) = 0$$

$$\eta_{nm} = \sqrt{\frac{U_{nm}^2}{a^2} - k^2} \approx \frac{U_{nm}}{a}, \text{ where } J_n(U_{nm}) = 0$$

The first few values of v_{nm} and u_{nm} are as follows:

$u_{01} = 2.405$	$v_{11} = 1.841$
$u_{11} = 3.832$	$v_{21} = 3.05$
$u_{21} = 5.136$	$v_{01} = 3.832$
$u_{02} = 5.520$	$v_{12} = 5.33$
$u_{12} = 7.010$	$v_{02} = 7.016$

From the above values of u_{nm} and v_{nm} it is at once apparent that maximum purity of mode can be achieved by exciting the TE_{11} mode, and eliminating the TE_{01} , TE_{21} , and TM_{01} modes through symmetry considerations.

Consider the exciting current distribution in a plane perpendicular to the axis of the cylinder, Fig. 3. Assume that corresponding to every current element, $\underline{J}_1(r_o, \theta, \alpha)$ where r_o is the distance of the element from the axis of the cylinder, θ is the angular displacement of its position vector with respect to the x-axis, and α is the angle between \underline{J}_1 and the x-axis, there exist corresponding current elements, $\underline{J}_2(r_o, \pi - \theta, -\alpha)$, $\underline{J}_3(r_o, \pi + \theta, \alpha)$, $\underline{J}_4(r_o, 2\pi - \theta, -\alpha)$.

Then, it immediately follows that

$$\int \underline{J} \cdot \underline{n}_{nm}^e d\tau = \int \underline{J} \cdot \underline{m}_{nm}^e d\tau = 0 \text{ for } n \text{ even}$$

Further, if corresponding to a positive z-component of current at $(r_o, 2\pi - \theta)$ and (r_o, θ) , there exist equal negative z-components of current at $(r_o, \pi - \theta)$ and $(r_o, \pi + \theta)$, then

$$\int \underline{J} \cdot \underline{p}_{nm}^e d\tau = 0, \text{ for } n \text{ even}$$

In general, if the exciting current symmetry is such that the distribution for $x < 0$ is the negative mirror image of that for $x > 0$, and if the distribution for $y < 0$ is the positive mirror image of that for $y > 0$, then only those modes will be excited for which n is odd.

A convenient index of attenuator performance is the percentage error made in a measurement of voltage as a function of the distance between exciting and receiving coils. The computed value of this error at 500 megacycles per second is shown by curves a and b in Fig. 4 for an attenuator with symmetrical and unsymmetrical receiving and exciting loops, (Fig. 5). Fig. 4 shows that a symmetrical exciting source permits a considerable decrease in the insertion loss, for a given accuracy tolerance, over that of an unsymmetrically excited attenuator.

4. Attenuators of Rectangular Cross-Section

Attenuators of rectangular cross-section may be treated similarly to those of circular cross-section. For a rectangular cavity, whose x, y, z, dimensions are a, b, c, with the origin of coordinates taken at a corner, the normalized vector wave function of zero curl is

$$\underline{E}_{lmn} = \sqrt{\frac{8}{abc}} \frac{1}{\sqrt{\frac{l^2}{a^2} + \frac{m^2}{b^2} + \frac{n^2}{c^2}}} \left[\frac{1}{a} \cos \frac{l\pi x}{a} \sin \frac{m\pi y}{b} \sin \frac{n\pi z}{c} \underline{i} + \frac{m}{b} \sin \frac{l\pi x}{a} \cos \frac{m\pi y}{b} \sin \frac{n\pi z}{c} \underline{j} + \frac{n}{c} \sin \frac{l\pi x}{a} \sin \frac{m\pi y}{b} \cos \frac{n\pi z}{c} \underline{k} \right] \quad (18)$$

The two independent normalized vector wave functions of zero divergence are

$$\underline{H}_{lmn} = \sqrt{\frac{8}{abc}} \frac{1}{\sqrt{\frac{l^2}{a^2} + \frac{m^2}{b^2}}} \left[-\frac{m}{b} \sin \frac{m\pi y}{b} \cos \frac{l\pi x}{a} \underline{i} + \frac{1}{a} \sin \frac{l\pi x}{a} \cos \frac{m\pi y}{b} \underline{j} \right] \sin \frac{n\pi z}{c} \quad (19)$$

and $\underline{N}_{lmn} = \sqrt{\frac{8}{abc}} \frac{1}{\sqrt{\frac{l^2}{a^2} + \frac{m^2}{b^2} + \frac{n^2}{c^2}}} \frac{1}{\sqrt{\frac{l^2}{a^2} + \frac{m^2}{b^2}}} \frac{1}{\sqrt{1 + \delta_o^n}} \left[-\frac{ln}{ac} \cos \frac{l\pi x}{a} \sin \frac{m\pi y}{b} \sin \frac{n\pi z}{c} \underline{i} - \frac{mn}{bc} \sin \frac{l\pi x}{a} \cos \frac{m\pi y}{b} \sin \frac{n\pi z}{c} \underline{j} + \left(\frac{l^2}{a^2} + \frac{m^2}{b^2} \right) \sin \frac{l\pi x}{a} \sin \frac{m\pi y}{b} \cos \frac{n\pi z}{c} \underline{k} \right]$

Again, when we solve for the field excited by a distribution of current, $\underline{J}(\underline{r}')$, part of the field developed into N_{lmn} functions exactly cancels that part of the field whose curl is zero, so that the resultant field, \underline{E} , may be expressed as the sum of transverse electric and transverse magnetic components.

$$\underline{E} = \underline{E}_{TE} + \underline{E}_{TM}$$

where $\underline{E}_{TE} = \frac{4j\omega\mu}{ab} \int \underline{J}(\underline{r}') \cdot \sum_{lm} \frac{\alpha_{lm}(\underline{r}') \alpha_{lm}(\underline{r}) \sinh \eta z'}{\eta_{lm} \left(\frac{1^2}{a^2} + \frac{m^2}{b^2} \right)} \left[\frac{e^{-\eta z}}{1 - e^{-2\eta c}} (1 - e^{-2\eta(c-z)}) \right] d\underline{r}'$

$$\alpha_{lm} = \left[-\frac{m}{b} \sin \frac{m\pi y}{b} \cos \frac{l\pi x}{a} \underline{j} + \frac{1}{a} \sin \frac{l\pi x}{a} \cos \frac{m\pi y}{b} \underline{j} \right]$$

and

$$\eta_{lm} = \sqrt{\left(\frac{l\pi}{a} \right)^2 + \left(\frac{m\pi}{b} \right)^2 - k^2}$$

$$\underline{E}_{TM} = \frac{-4j}{\omega\epsilon ab} \int \underline{J}(\underline{r}') \cdot \sum_{lm} \frac{e^{-\eta z}}{1 - e^{-\eta c}} \left\{ \frac{\underline{S}(\underline{r}') \underline{S}(\underline{r}) \eta \sinh \eta z'}{\left(\frac{1^2}{a^2} + \frac{m^2}{b^2} \right)} + \pi \underline{q}_l(\underline{r}') \underline{S}(\underline{r}) \cosh \eta z' \right\} (1 - e^{-2\eta(c-z)})$$

$$- \left\{ \pi \underline{S}(\underline{r}') \underline{q}_l(\underline{r}) \sinh \eta z' + \pi^2 \left(\frac{1^2}{a^2} + \frac{m^2}{b^2} \right) \underline{q}_l(\underline{r}') \frac{\underline{q}_l(\underline{r}) \cosh \eta z'}{\eta} \right\} (1 + e^{-2\eta(c-z)}) d\underline{r}'$$

$$\text{where } S_{lm} = \left[\frac{1}{a} \cos \frac{l\pi x}{a} \sin \frac{m\pi y}{b} + \frac{m}{b} \sin \frac{l\pi x}{a} \cos \frac{m\pi y}{b} \right]$$

$$Q_{lm} = \sin \frac{l\pi x}{a} \sin \frac{m\pi y}{b} - k$$

r' and r refer respectively to the position coordinates of J , and the point at which the field is evaluated.

It will be noticed that E_{TE} and E_{TM} have the same value of attenuation constant, for the same mode numbers, l , m .

Also, we shall assume that the receiving coil is rigidly fixed to the movable end of the cavity, so that the factor $(1 \pm e^{-2\eta(c-z)})$ is cancelled out in the measurement of the ratio of any two voltages. The magnitude of the error introduced by the factor $(1 - e^{-2\eta c})$ is such, that if the smallest value of c used is always greater than 1.5 times the larger dimension of cross-section, the factor will introduce an error of less than 1 part in 10,000 for the TE_{01} mode, and less for higher modes.

One advantage of an attenuator tube with rectangular cross-section over that with circular cross-section is that for the former, there is no need to discriminate between TE and TM type modes, for the same index numbers, l , m , since for given values of l and m , the voltage

induced in the collecting coil will vary as $e^{-\sqrt{\frac{\pi^2 l^2}{a^2} + \frac{\pi^2 m^2}{b^2} - k^2} Z}$

for TM and TE type modes, alike. Of course, for tubes of circular cross-section, this is not true, except for cases of accidental degeneracy.

Further, for tubes of rectangular cross-section, it is possible to secure greater suppression of unwanted modes by a suitable choice of ratio of the two dimensions of cross-section. The following table enumerates the ratio of attenuation constants for various modes to that of the lowest mode, for various ratios of rectangular cross-section dimensions and for circular cross-section.

Table 1

Rectangular Waveguide					Circular Waveguide	
Mode	$\frac{\eta}{\eta_{TE_{01}}}$	$\frac{\eta}{\eta_{TE_{01}}}$	$\frac{\eta}{\eta_{TE_{01}}}$	$\frac{\eta}{\eta_{TE_{01}}}$	$\frac{\eta}{\eta_{TE_{11}}}$	Mode
	a=b	a=0.9b	a= $\frac{b}{2}$	a= $\frac{b}{3}$		
TE ₀₁	1	1	1	1	1	TE ₁₁
TE ₀₂	2	2	2	2	1.31	TM ₀₁
TE ₀₃	3	3	3	3	1.66	TE ₂₁
TE ₁₀	1	1.1	2	3	2.08	TE ₀₁ , TM ₁₁
TE ₂₀	2	2.2	4	6	2.79	TM ₂₁
TE ₁₁ , TM ₁₁	1.41	1.5	2.2	3.1	2.90	TE ₁₂
TE ₂₁ , TM ₂₁	2.2	2.4	4.1	6.1	3.0	TM ₀₂

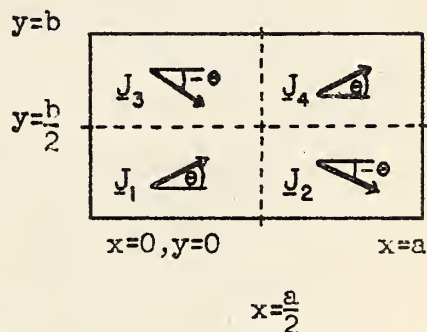
It becomes apparent that the optimum practical ratio in the above table is $\frac{b}{a} = 3$, and that this choice allows the unwanted modes to decay much faster than for circular cross-section.

If the exciting current distribution is chosen, so that to each element of current corresponds its negative mirror image with respect to the plane $x = \frac{a}{2}$, and its positive mirror image with respect to the plane $y = \frac{b}{2}$, then it is easily seen that

$$\left. \begin{aligned} \int J(\kappa') \cdot \underline{\alpha}_{lm} d\tau' \\ \int J(\kappa') \cdot \underline{s}_{lm} d\tau' \\ \int J(\kappa') \cdot \underline{q}_{lm} d\tau' \end{aligned} \right\} = 0, \text{ for } l \text{ odd or } m \text{ even}$$

We shall prove the first of the above three equations. Proof of the other two may be carried out similarly.

Consider a current element, $J_1(x', y', z')$, situated at (x', y', z') , making an angle θ with the x-axis. Then its negative mirror image with respect to the plane $x = \frac{a}{2}$, call it J_2 , is situated at $(a-x', y', z')$, making an angle $-\theta$ with the x-axis. Also J_3 , positive mirror image of J_1 with respect to the plane $y = \frac{b}{2}$ is situated at $(x', b-y', z')$ and makes an angle $-\theta$ with respect to the x-axis.



Similarly, J_4 , situated at $(a-x', b-y', z')$, the positive mirror image of J_2 with respect to the plane $y = \frac{b}{2}$ makes an angle θ with the x-axis.

$$\int \underline{\alpha}_{lm} d\tau' = \int \sum_{l=1}^4 J_l \cdot \left[\frac{-m}{b} \sin \frac{m\pi y'}{b} \cos \frac{l\pi x'}{a} + \frac{l}{a} \sin \frac{l\pi x'}{a} \cos \frac{m\pi y'}{b} \right] d\tau'$$

On substituting the positional coordinates corresponding to each current element, we get

$$\int J_{lm} \alpha d\tau' = \int |J| \left\{ -m \frac{\cos \theta}{b} \left[\sin \frac{m\pi y'}{b} + \sin \frac{m\pi(b-y')}{b} \right] \left[\cos \frac{l\pi x'}{a} + \cos \frac{l\pi(a-x')}{a} \right] \right. \\ \left. + \frac{1}{a} \sin \theta \left[\sin \frac{l\pi x'}{a} - \sin \frac{l\pi(a-x')}{a} \right] \left[\cos \frac{m\pi y'}{b} - \cos \frac{m\pi(b-y')}{b} \right] \right\} d\tau'$$

If we substitute in the above the trigonometric identities,

$$\cos \frac{l\pi x'}{a} + \cos \frac{l\pi(a-x')}{a} = 2 \cos \frac{l\pi}{2} \cos \left(\frac{l\pi x'}{a} - \frac{l\pi}{2} \right)$$

$$\sin \frac{l\pi x'}{a} - \sin \frac{l\pi(a-x')}{a} = 2 \cos \frac{l\pi}{2} \sin \left(\frac{l\pi x'}{a} - \frac{l\pi}{2} \right)$$

$$\sin \frac{m\pi y'}{b} + \sin \frac{m\pi(b-y')}{b} = 2 \sin \frac{m\pi}{2} \cos \left(\frac{m\pi y'}{b} - \frac{m\pi}{2} \right)$$

$$\cos \frac{m\pi y'}{b} - \cos \frac{m\pi(b-y')}{b} = -2 \sin \frac{m\pi}{2} \sin \left(\frac{m\pi y'}{b} - \frac{m\pi}{2} \right)$$

we finally get,

$$\int J_{lm} \alpha d\tau' = -4 \sin \frac{m\pi}{2} \cos \frac{l\pi}{2} \int |J| \left[\frac{m \cos \theta}{b} \cos \left(\frac{m\pi y'}{b} - \frac{m\pi}{2} \right) \cos \left(\frac{l\pi x'}{a} - \frac{l\pi}{2} \right) \right. \\ \left. + \frac{1}{a} \sin \theta \sin \left(\frac{l\pi x'}{a} - \frac{l\pi}{2} \right) \sin \left(\frac{m\pi y'}{b} - \frac{m\pi}{2} \right) \right] d\tau'$$

Accordingly,

$$\int J_{lm} \alpha d\tau' = 0, \text{ for } l \text{ odd, or } m \text{ even.}$$

The advantages of employing this type of symmetrical source distribution become apparent when we consult Table 1, and recognize that it eliminates four out of the first six spurious modes.

Another advantage of rectangular attenuators over those of circular cross-section is the ease with which current distributions of slightly higher symmetry may be used to eliminate further spurious modes, by placing the current elements at the nodal points of the undesired modes. The relative voltage error for a rectangular attenuator with a simple symmetric loop source, and a double loop source, (Fig. 6) whose Y dimension is so chosen that modes for which $m = 3$ are not excited, is graphed in Fig. 4.

Attenuators for use at 20 to 30 megacycles per second with circular and rectangular cross-sections have been constructed for testing the theoretical conclusions given in this report. Fig. 7 illustrates a tentative design employing rectangular guide. The application of the principles of symmetry discussed above is illustrated in the design of the coils, (Fig. 8) used with the circular type attenuator.

These attenuators can also be used for microwave attenuation measurements by means of the heterodyne substitution method, wherein an unknown attenuator in an r-f channel is compared against the standard attenuator used in an i-f channel.

5. Conclusion

It may be concluded, in general, then, that attenuators of rectangular cross-section have two advantages over those of circular cross-section.

1. Greater symmetry with respect to the dominant mode in the rectangular guide permit one to eliminate more spurious modes.

2. A slight departure from symmetry in the rectangular guide is not so serious as in the circular guide, since the spurious modes decay more rapidly in the former.

Opportunity is taken here to thank Dr. Harold Lyons for his interest and helpful discussions during the course of this investigation.

Appendix I

$$1 \quad \text{Let } S_1 = \sum_{l=1}^{\infty} \frac{\sin \frac{l\pi z'}{d} \sin \frac{l\pi z}{d}}{\gamma^2 + \frac{l^2 \pi^2}{d^2}} = \frac{d^2}{\pi^2} \sum_{l=1}^{\infty} \frac{\sin \frac{l\pi z'}{d} \sin \frac{l\pi z}{d}}{\frac{d^2 \gamma^2}{\pi^2} + l^2}$$

$$2 \quad \text{Let } \frac{d\gamma}{\pi} = \beta$$

$$3 \quad S_1 = \frac{d^2}{2\pi^2} \sum_{l=1}^{\infty} \frac{\cos \frac{l\pi}{d} (z-z') - \cos \frac{l\pi}{d} (z+z')}{\beta^2 + l^2} = \frac{d^2}{4\pi^2} \sum_{l=-\infty}^{\infty} \frac{\cos \alpha l - \cos \alpha' l}{\beta^2 + l^2}$$

$$4 \quad \text{where } \alpha = \frac{\pi(z-z')}{d}, \quad \alpha' = \frac{\pi(z+z')}{d}$$

$$5 \quad \text{Consider } f(z) = \frac{e^{j\alpha z}}{(z^2 + Z^2)(e^{2\pi j Z} - 1)} \quad \text{let } Z = R(\cos \theta + j \sin \theta)$$

Then $\lim_{R \rightarrow \infty} |Zf(z)| = 0$, and $\lim_{R \rightarrow \infty} zf(z) = 0$, provided $0 \leq \alpha \leq 2\pi$.

Then, ⁽⁷⁾ the line-integral of $f(z)$ around an infinite circle enclosing the complex plane vanishes.

$$6 \quad \lim_{R \rightarrow \infty} \oint f(z) dz = 0$$

Since $f(z)$ has poles at $\pm j\beta, 0, \pm 1, \pm 2, \dots$,

$$7 \quad 0 = \sum_{l=-\infty}^{l=\infty} \frac{e^{j\alpha l}}{\beta^2 + l^2} + \frac{\pi}{\beta} \left\{ \frac{e^{-\alpha\beta}}{e^{-2\pi\beta} - 1} - \frac{e^{\alpha\beta}}{e^{2\pi\beta} - 1} \right\}$$

$$8 \quad \text{or } \sum_{l=-\infty}^{\infty} \frac{\cos \alpha l}{\beta^2 + l^2} = \frac{\pi}{\beta} \left[\frac{e^{\alpha\beta}}{e^{2\pi\beta} - 1} - \frac{e^{-\alpha\beta}}{e^{-2\pi\beta} - 1} \right]$$

On substituting (8) in (3), with a little algebra we get immediately

$$9 \quad S_1 = \frac{d}{2\gamma} \frac{\sinh \gamma z' (1 - e^{-2\gamma(d-z)})}{1 - e^{-2\gamma d}} e^{-\gamma z}$$

Appendix II

$$1 \quad \text{Let } S_2 = \sum_{l=0}^{\infty} \frac{\frac{1}{d} \pi \sin \frac{1}{d} \pi z' \cos \frac{1}{d} \pi z}{\gamma^2 + \left(\frac{1}{d} \pi\right)^2}$$

$$2 \quad \text{Then } S_2 = \frac{d}{dz'} S_1 = -\frac{d}{2} \sinh \gamma z' \left[\frac{e^{\gamma z}}{e^{2\gamma d} - 1} - \frac{e^{-\gamma z}}{e^{-2\gamma d} - 1} \right]$$

$$3 \quad \text{Let } S_3 = \sum_{l=1}^{\infty} \frac{\frac{1}{d} \pi \cos \frac{1}{d} \pi z' \sin \frac{1}{d} \pi z}{\gamma^2 + \left(\frac{1}{d} \pi\right)^2}$$

$$4 \quad \text{Then } S_3 = \frac{d}{dz'} S_1 = -\frac{d}{2} \cosh \gamma z' \left[\frac{e^{\gamma z}}{e^{2\gamma d} - 1} + \frac{e^{-\gamma z}}{e^{-2\gamma d} - 1} \right]$$

$$5 \quad \text{Let } S_4 = \sum \frac{\left(\frac{1}{d} \pi\right)^2 \cos \frac{1}{d} \pi z \cos \frac{1}{d} \pi z'}{\gamma^2 + \left(\frac{1}{d} \pi\right)^2}$$

$$6 \quad \text{Then } S_4 = \frac{d}{dz'} S_2 = \frac{-\gamma d}{2} \cosh \gamma z' \left[\frac{e^{\gamma z}}{e^{2\gamma d} - 1} - \frac{e^{-\gamma z}}{e^{-2\gamma d} - 1} \right]$$

REFERENCES

1. Harnett and Case, IRE, Vol. 23, p.578, June 1935. "The Design and Testing of Multirange Receivers".
2. Deutsche Mathematiker - Vereinigung Jahresbericht, Vol. 21, p.309, 1912.
3. Heitler, "Quantum Theory of Radiation", Revised 1944, p.47.
4. Condon, E. U., Rev. Mod. Phys. Oct. 1942, p.341.
5. Stratton, J. A., Electromagnetic Theory, p.465.
6. Stratton, J. A., ibid, p.392.
7. McRobert, T. M., "Functions of a Complex Variable", MacMillan Co. 1933, p.115.

September 23, 1946

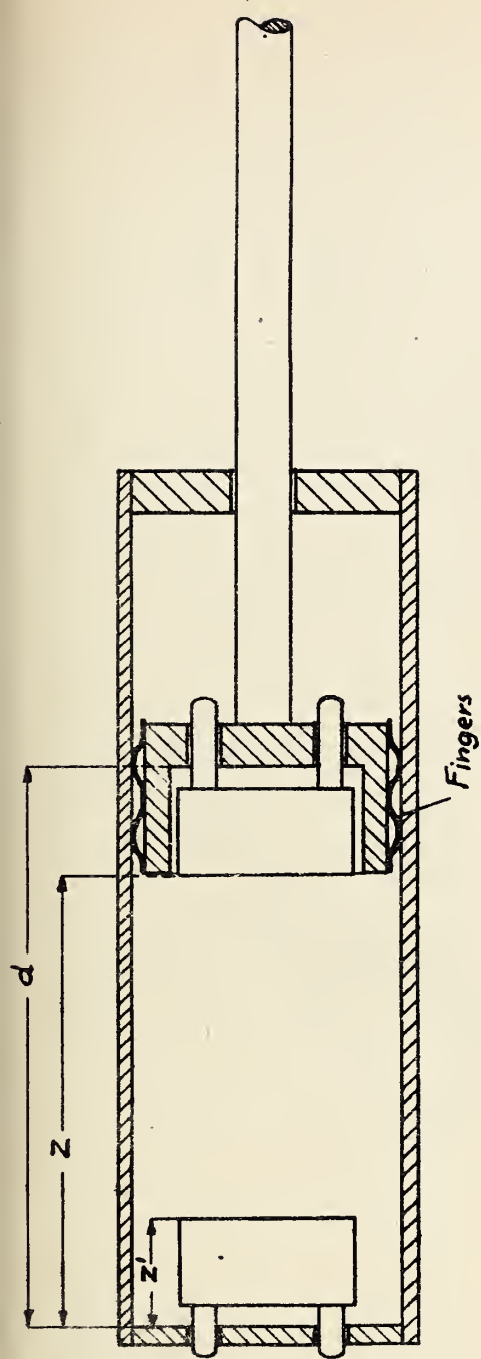


Fig. 1. Schematic of attenuator.

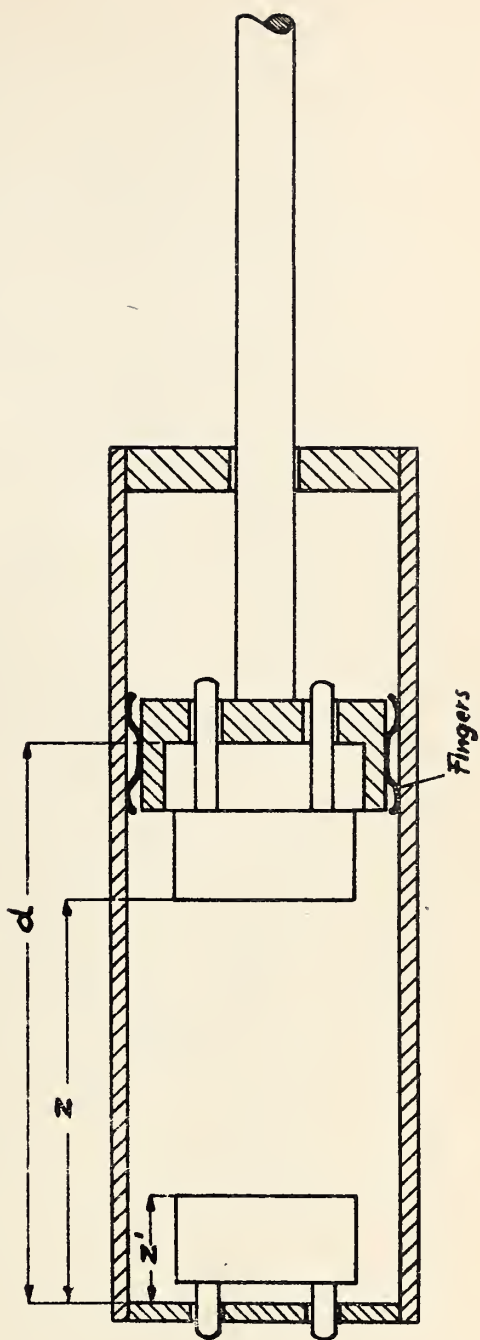
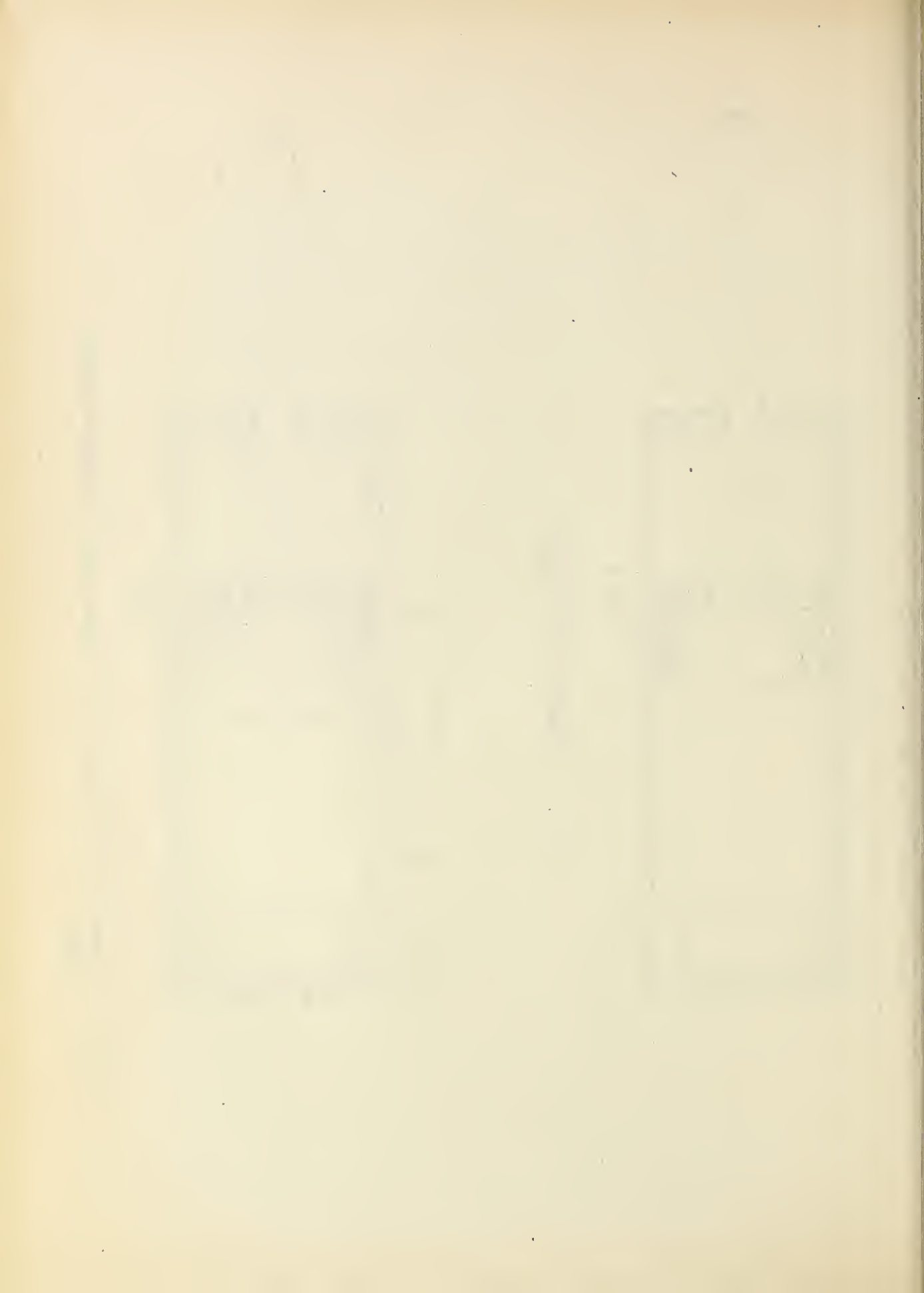


Fig. 2. Schematic of attenuator with sliding contact behind receiving loop.



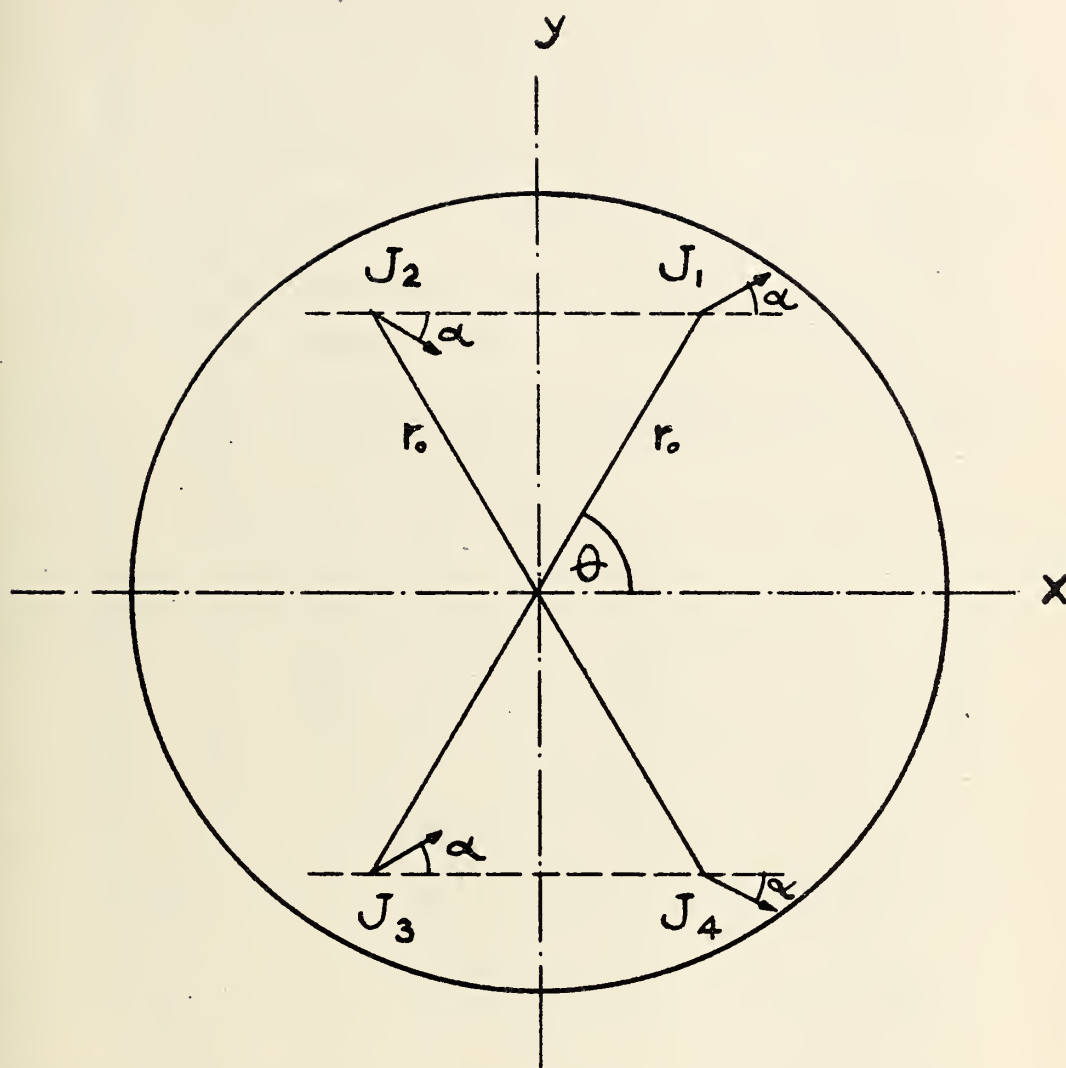


Fig. 3. Current distribution in plane perpendicular to axis of cylinder.

Voltage Attenuation in decibels

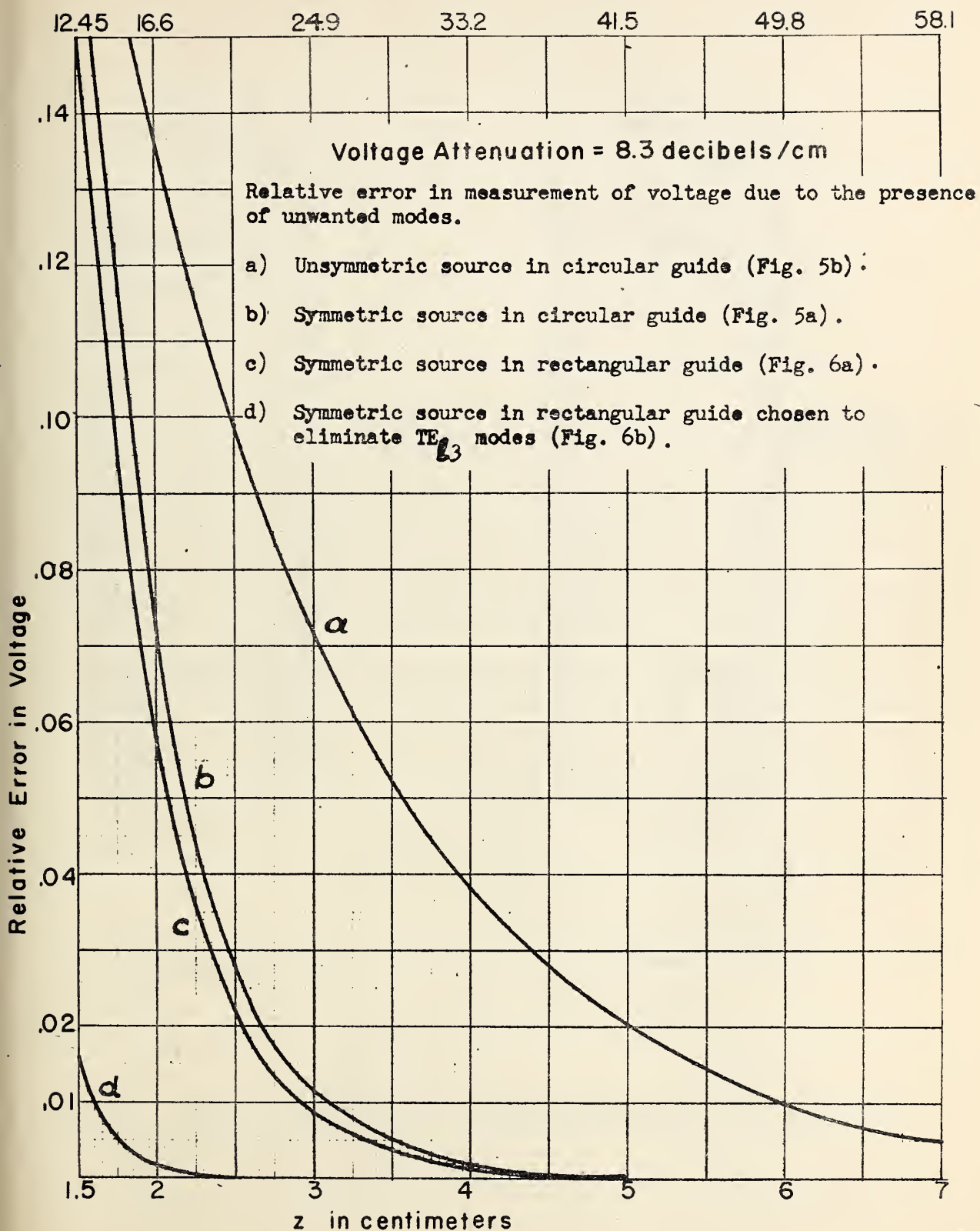
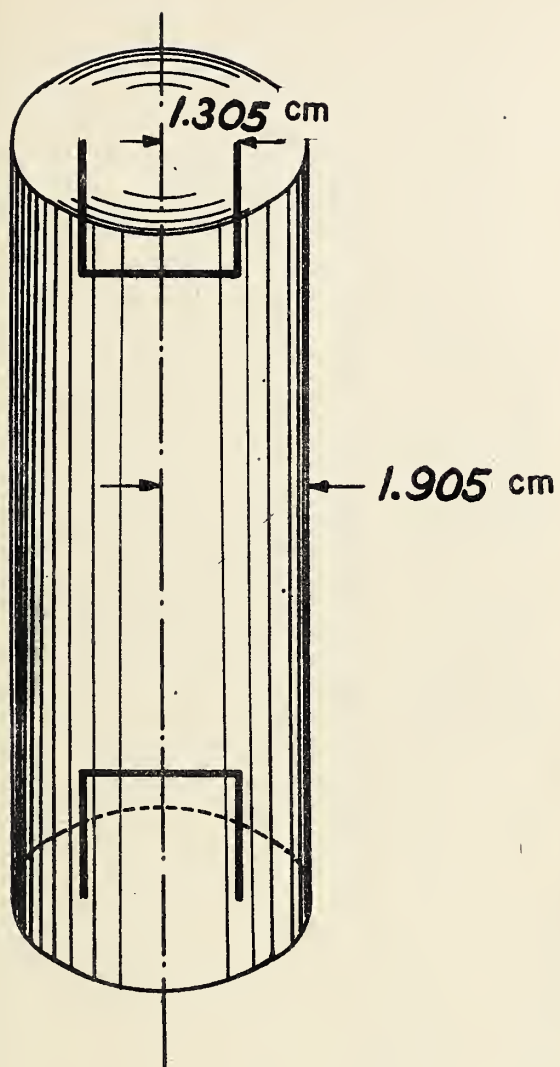
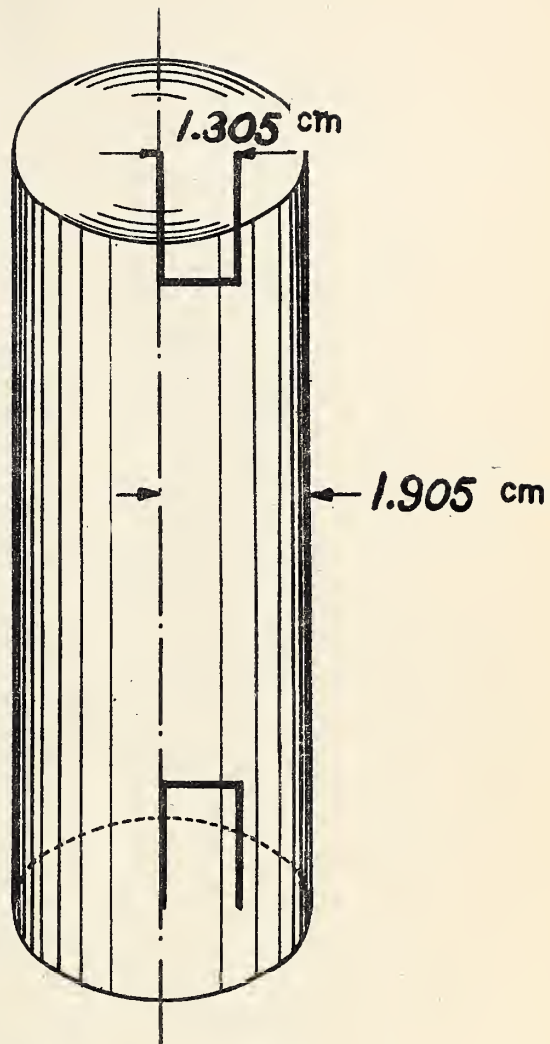


Fig. 4.





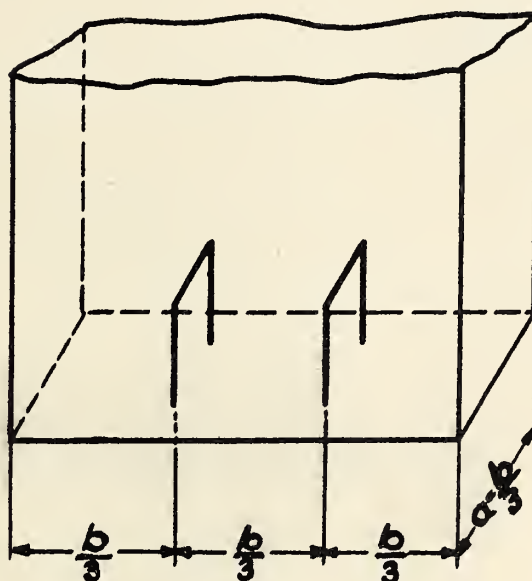
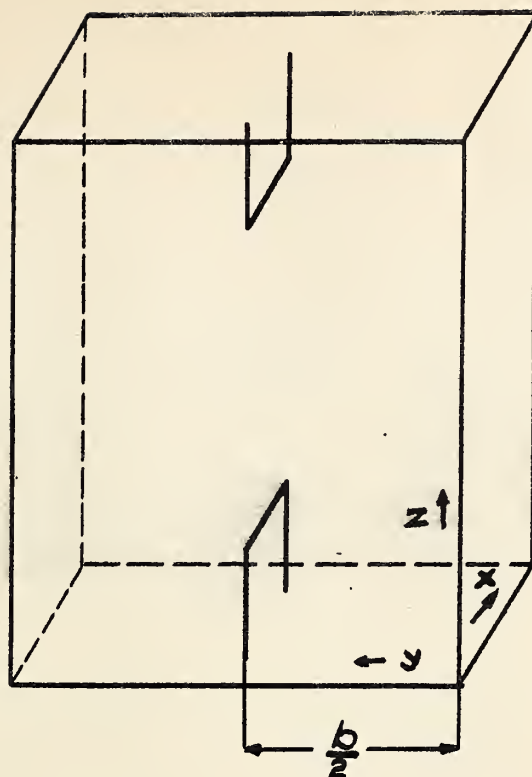
b) Symmetric loop.



a) Unsymmetric loop.

Fig. 5. Schematic of exciting and receiving loops in circular guide.

a) Symmetric loop.



b) Symmetric double loop placed at nodes so that no modes are excited for which $m \neq 3$.

Fig. 6. Schematic of exciting and receiving loops in rectangular guide.



THE UNIVERSITY OF CHICAGO PRESS



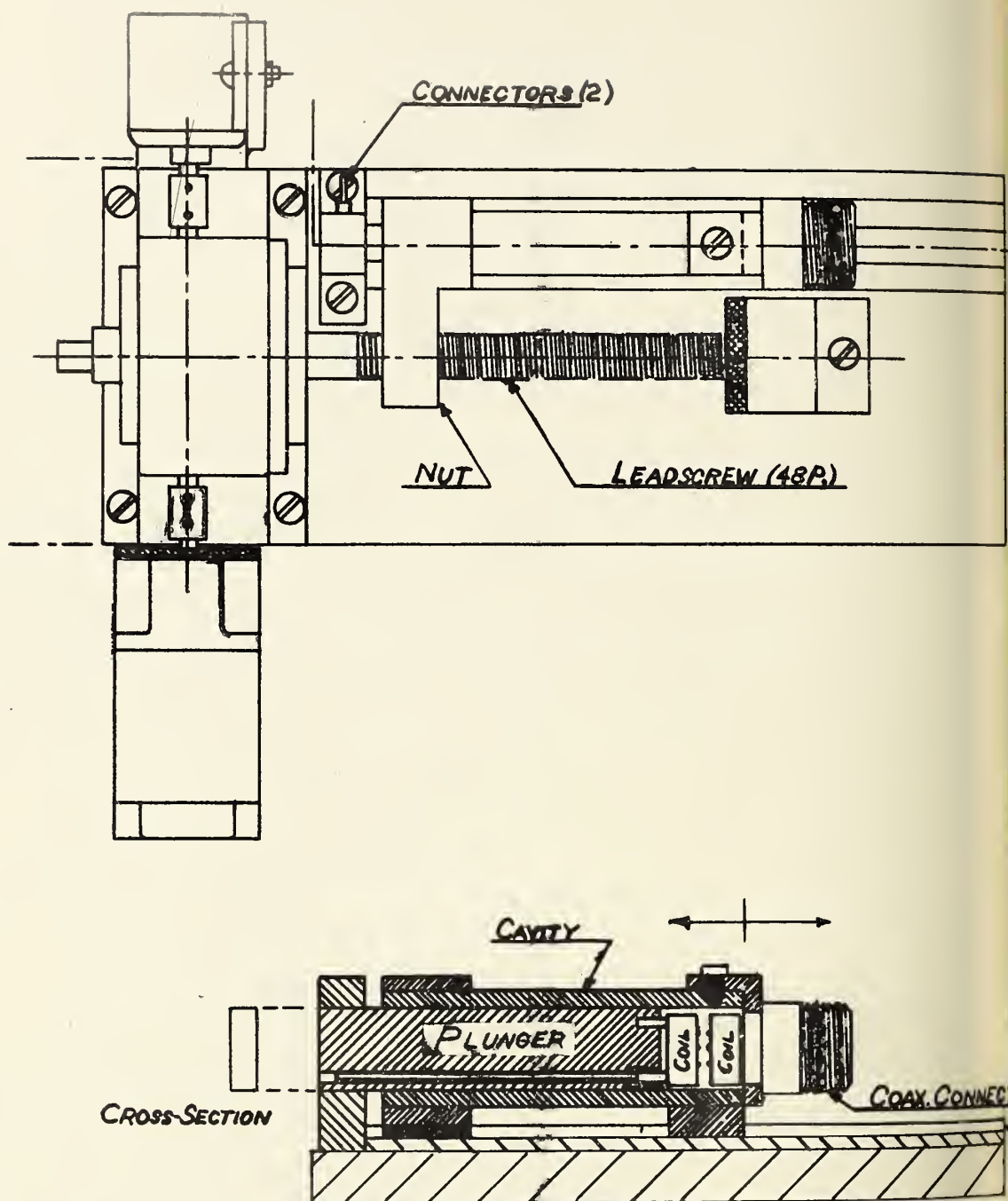
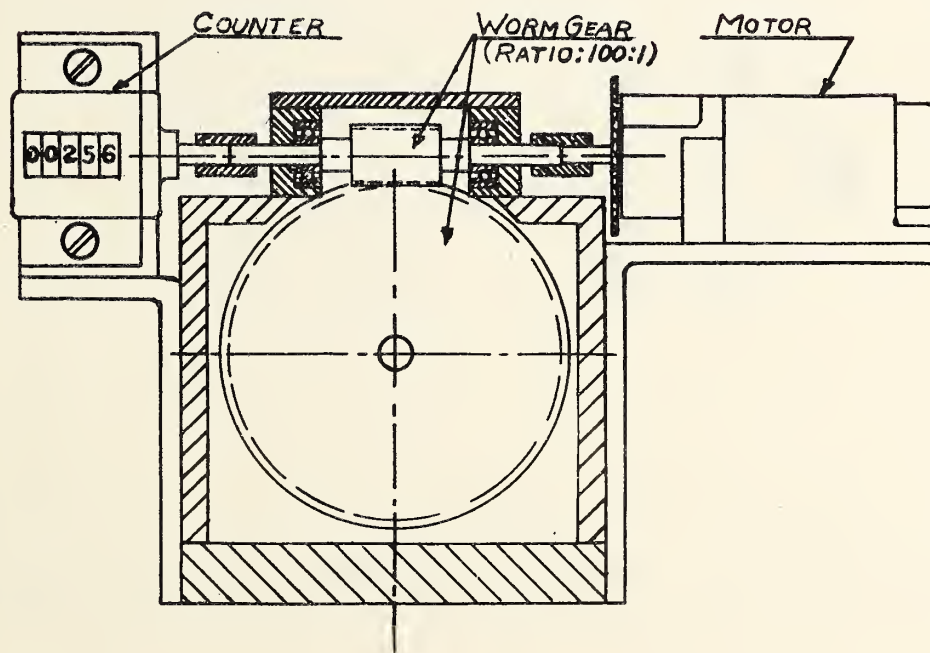


Fig. 7. Assembly

CUTOFF ATTENUATOR WITH RECTANGULAR CROSS-SECTION



ctagular attenuator .

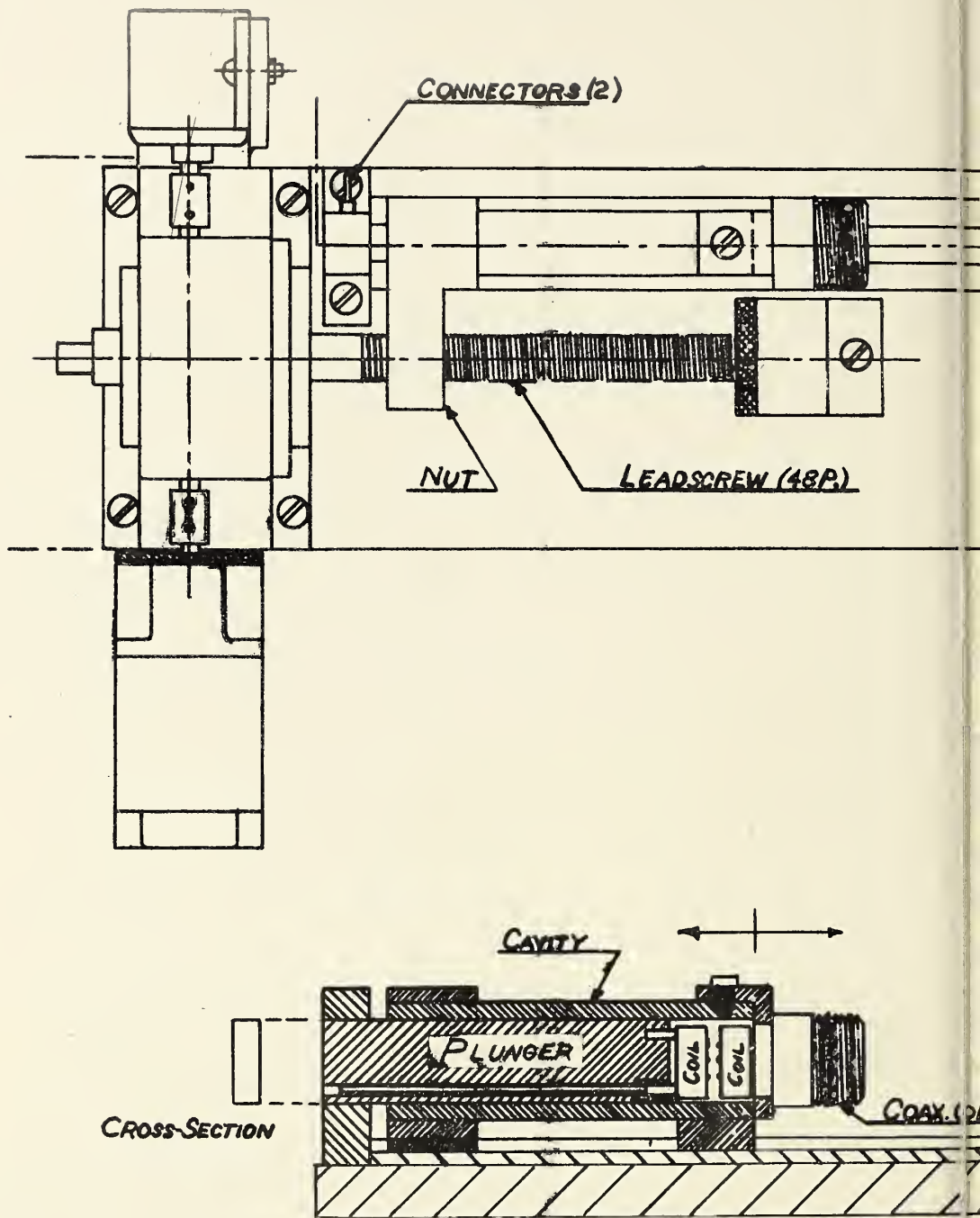
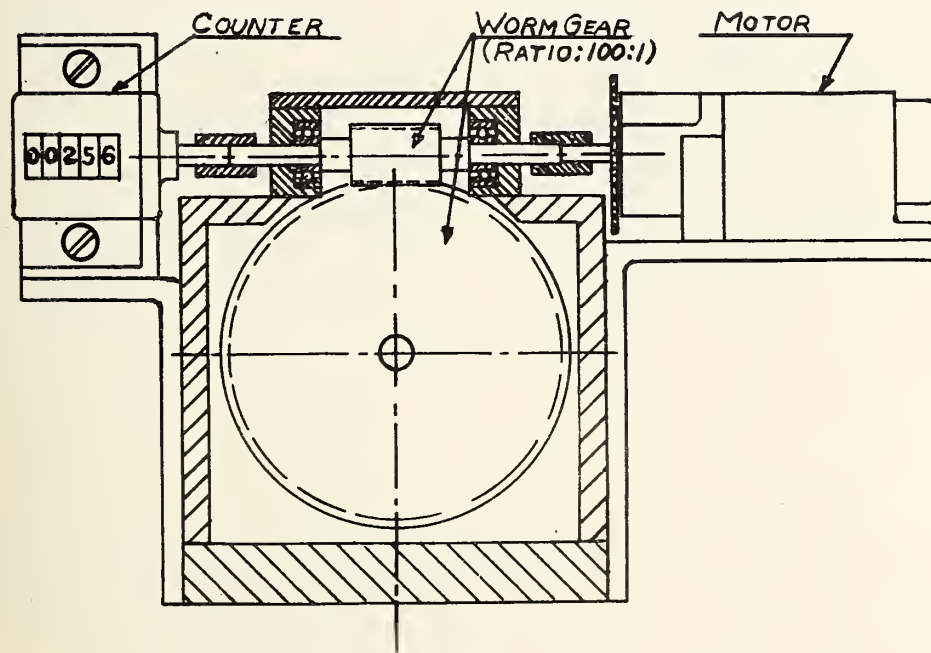


Fig. 7.

CUTOFF ATTENUATOR WITH RECTANGULAR CROSS-SECTION



rectangular attenuator .

EXCITER COIL PT. 8A

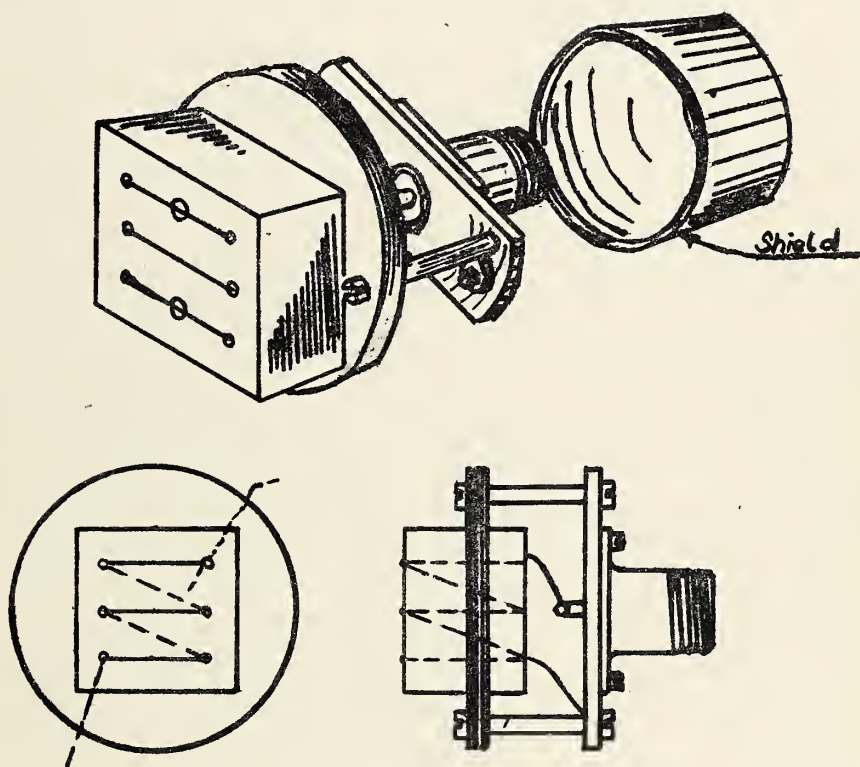


Fig. 8. Perspective drawing of coil forms for circular attenuator .



